Ultraino: An Open Phased-Array System for Narrowband Airborne Ultrasound Transmission

Asier Marzo, Tom Corkett, and Bruce W. Drinkwater

***Abstract*— Modern ultrasonic phased-array controllers are electronic systems capable of delaying the transmitted or received signals of multiple transducers. Configurable transmit–receive array systems, capable of electronic steering and shaping of the beam in near real-time, are available commercially, for example, for medical imaging. However, emerging applications, such as ultrasonic haptics, parametric audio, or ultrasonic levitation, require only a small subset of the capabilities provided by the existing controllers. To meet this need, we present Ultraino, a modular, inexpensive, and open platform that provides hardware, software, and example applications specifically aimed at controlling the transmission of narrowband airborne ultrasound. Our system is composed of software, driver boards, and arrays that enable users to quickly and efficiently perform research in various emerging applications. The software can be used to define array geometries, simulate the acoustic field in real time, and control the connected driver boards. The driver board design is based on an Arduino Mega and can control 64 channels with a square wave of up to 17 Vpp and $\pi/5$ phase resolution. Multiple boards can be chained together to increase the number of channels. The 40-kHz arrays with flat and spherical geometries are demonstrated for parametric audio generation, acoustic levitation, and haptic feedback.**

***Index Terms*— Acoustic levitation, airborne, Arduino, open hardware, parametric audio, phased arrays, ultrasonic haptics, ultrasonics.**

I. Introduction

PHASED arrays are a collection of elements that transmit or receive with specific phases or time delays. They are in widespread use in radar [1], sonar [2], and ultrasonic imaging [3] since they can dynamically steer and shape the beam. Recently, various nontraditional applications that require the use of transmit-only airborne and narrowband ultrasound have emerged; these applications include acoustic levitation [4], mid-air tactile feedback [5], wireless power transfer [6], and parametric audio generation [7]. However, currently available systems are either very high specification [8]–[10] and hence expensive, or fully integrated into a commercial product (e.g., Ultrahaptics, U.K.; Pixie Dust Tech., Japan). Neither option provides researchers and developers with a suitable platform to explore these emerging applications.

Manuscript received September 28, 2017; accepted October 30, 2017. Date of publication November 2, 2017; date of current version January 1, 2018. This work was supported by the UK Engineering and Physical Science Research Council under Grant EP/N014197/1. *(Corresponding author: Asier Marzo.)*

A. Marzo and B. W. Drinkwater are with the Mechanical Engineering Department, Bristol University, Bristol BS8 1TR, U.K. (e-mail: amarzo@hotmail.com; mebwd.@.bristol.ac.uk).

T. Corkett is with the Electronic Engineering Department, Bristol University, Bristol BS8 1TR, U.K. (e-mail: tc13617@my.bristol.ac.uk).

This paper has supplementary downloadable material available at http://ieeexplore.ieee.org., provided by the author.

Digital Object Identifier 10.1109/TUFFC.2017.2769399

In this paper, we present Ultraino, an open platform consisting of software for designing and controlling arrays and beams along with hardware to develop narrowband transmit-only applications. Unlike the existing solutions, Ultraino is open, modular, inexpensive, and simple enough to be assembled by most researchers. The narrowband airborne array system that we propose has applications in various active research fields such as acoustic levitation, wireless power transfer, mid-air ultrasonic haptic feedback, and parametric loudspeakers. We note that these are recent emerging nontraditional applications, so it is reasonable to anticipate further, yet unknown, applications of our system in the future years. The creation of this open platform will therefore allow a wide range of researchers from across the globe to explore these and other emerging applications, thereby lowering the barriers to research in this field and increasing the possibilities for innovation.

A. Related Work

The design of ultrasonic phased-array controllers is an active field. For instance, the RASMUS platform [8], [11] can transmit and receive with 1024 transducer elements and receive from 64 channels simultaneously at 40-MHz sampling with 12-b resolution; later, it was updated to the platform SARUS [12] capable of transmitting and receiving with 1024 elements simultaneously. Similarly, UARP [9], [13] is a high-speed transmit–receive system supporting up to 96 channels (UARP 2.0 will support 128 channels), emitting at 15 MHz and receiving at 50 MHz with 12-b resolution.

Apart from the above platforms developed by researchers, there are multiple commercial array controllers: Micropulse (PEAK NDT, U.K.), Vantage (Verasonics, WA, USA), or SonixTOUCH Research (Ultrasonix Medical Corporation, Canada) to name a few. Some commercial platforms provide access to the raw data [14]. However, commercial systems cannot always fulfill the requirement of researchers to access the data, embed new algorithms, or extend functionality as an open platform would do. To our knowledge, only one open platform for ultrasound array research has been described in the literature [10], [15], [16], ULA-OP is a powerful and portable ultrasonic array imaging system specifically developed for research purposes. It supports up to 256 elements and makes feasible the experimental testing of novel transmission strategies or challenging processing methods such as real-time vector Doppler schemes.

The above array systems facilitate both emission and reception of high-frequency ultrasound. Although more limited, there are also some examples aimed specifically at the

lower frequencies typical of airborne ultrasound. For instance, Harput *et al.* [17] developed a phased array with six emitters and four receivers working at 40 kHz, but the emitters were excited by a simple pulse and the number of channels is insufficient for the applications that we describe; also, no software is provided.

Ultrahaptics (Bristol, U.K.) is a company that sells phased arrays with 196-elements operating at 40 kHz for the generation of mid-air tactile sensations. These arrays are of high-quality but being a commercial solution, the software and hardware cannot be easily modified. Similarly, Pixie Dust Technologies (Tokyo, Japan) provides a parametric speaker based on phased arrays. However, similar to Ultrahaptics, this is a commercial solution for a specific application and thus it is hard to modify or adapt to the various requirements of the researchers.

B. Ultraino Overview

We focus on the requirements of an array system capable of the transmission of narrowband airborne ultrasound. Such a system does not require wide bandwidths on transmission or reception electronics or analog-to-digital-converters (ADCs) to receive the signals. Furthermore, the typical working frequency for airborne applications is in the range 20–100 kHz which does not necessitate complex electronics. We show that for a frequency of 40 kHz, low-cost electronic components and transducers are commercially available. Through a series of examples, we show that a relatively simple design of array control system is capable of effectively delivering these specifications and is therefore able to support research in various emerging ultrasound applications.

The system hardware consists of a driver board capable of reading the amplitude and phases produced by the software and then generating half-square wave driving signals of up to 17 Vpp and $\pi/5$ phase resolution for 64 individual channels. Up to 15 boards can be chained to increase the number of channels. A set of 64 phases can be updated 25 times per second. For complex and fast field modulations, it is also possible to upload onto the board up to 32 phase patterns and a script that exactly specifies how many periods each pattern should be emitted.

The software is multiplatform (i.e., can run directly in Windows, Linux, and MacOs) and allows users to define array geometries and then visualize the resulting acoustic fields. The software can calculate the phase and amplitudes of the transducers required for the chosen beamforming operations. If needed, acoustic radiation forces can also be calculated.

For a wide uptake of Ultraino, we provide source code, components list, PCB designs, as well as video instructions for assembling the board and example arrays for applications in particle levitation, mid-air ultrasonic haptics and parametric audio (Supplementary Movies and https://github.com/asiermarzo/Ultraino). A PC running the software, driver board, and an array are shown in Fig. 1.

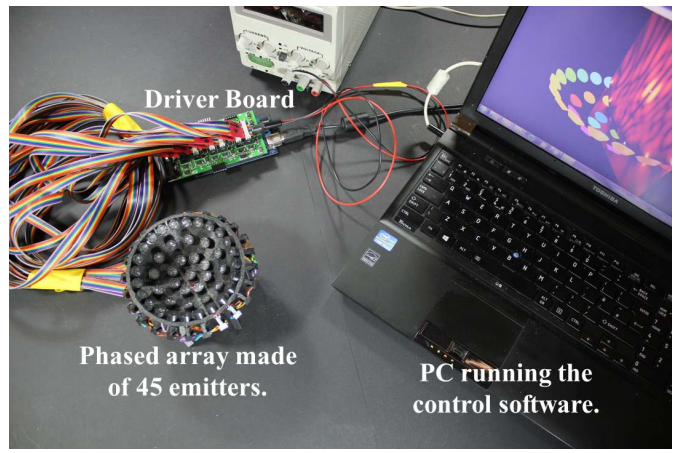

Fig. 1. Photograph containing all the components of the Ultraino system. A PC running the control software that can command the driver board and simulate the acoustic field in real time; a driver board capable of generating and amplifying up to 64 signals; and a spherical cap array made of 45 elements.

II. Methods

A. Models

To calculate the acoustic field in real time, we employed a single frequency far-field piston model of each transducer. While our simulation neglects reflections and nonlinear effects, its simplicity allows the software to be executed in real time which then facilitates the interactive exploration of the acoustic fields generated by any user-defined array.

The complex acoustic pressure P at point $\boldsymbol{r}$ due to a piston source [18] emitting at a single frequency can be modeled as

$$P(\boldsymbol{r}) = P_0 A \frac{D_f(\theta)}{d} e^{i(\varphi + kd)}$$

where P_0 is a constant that defines the transducer amplitude power and A is the peak-to-peak amplitude of the excitation signal. D_f is a far-field directivity function that depends on the angle θ between the transducer normal and $\boldsymbol{r}$. Here, $D_f = 2J_1(ka\sin\theta)/ka\sin\theta$, which is the directivity function of a circular piston source, where J_1 is a first-order Bessel function of the first kind and a is the piston radius. This directivity function can be simplified as $D_f = \mathrm{sinc}(ka\sin\theta)$. The term $1/d$ accounts for divergence, where d is the propagation distance in free space. $k = 2\pi/\lambda$ is the wavenumber and λ is the wavelength (8.6 mm in air at 25 °C). φ is the initial phase of the piston. For an array of multiple piston sources, the total field can be obtained by summation of the contribution from each source.

To calculate the force exerted on a sphere due to a complex pressure field, we can use the negative gradient of the Gork'ov potential [19], [20] $\boldsymbol{F} = -\nabla U$

$$U = 2K_1(|p|^2) - 2K_2(|p_x|^2 + |p_y|^2 + |p_z|^2)$$

$$K_1 = \frac{1}{4}V\left(\frac{1}{c_0^2\rho_0} - \frac{1}{c_s^2\rho_s}\right)$$

$$K_2 = \frac{3}{4}V\left(\frac{\rho_0 - \rho_s}{\omega^2\rho_0(\rho_0 + 2\rho_s)}\right)$$

where V is the volume of the spherical particle, ω is the frequency of the emitted waves, ρ is the density, and c is the speed of sound (with the subscripts 0 and s referring to the host medium and the solid particle material, respectively).

p is the complex pressure and p_x, p_y, p_z are, respectively, its spatial derivates over x, y, and z.

For our system, $P_0 = 0.17$ Pa at 1 m per Vpp of a square excitation signal, $a = 4.5$ mm. Air host medium, $\rho_0 = 1.18$ Kg/m^3, and $c_0 = 346$ m/s. Expanded Polystyrene (EPS) particles $\rho_s = 900$ m/s and $c_s = 29$ Kg/m^3.

B. Software

The software permits users to define the geometry of the array; i.e., the position and orientation of each transducer as well as their output amplitude and phase. The user is also able to select transducers with different frequencies and apertures. Once the user has defined the array geometry, they can select a predefined beamforming operation, e.g., focusing or generating a trap at a specific point in space. The software calculates the single-frequency complex acoustic field (i.e., amplitude and phase) emitted by the array (using the algorithms described in more detail in Section II-A). The field is presented in the form of 2-D slices through the 3-D field. A slice of 1024×800 for a 256 elements array was calculated in 40 ms using an Intel i5 with an integrated graphics processing unit, so the acoustic fields appear to the user in real time. This aids the acoustic design process as, for example, the focal point can be dragged with the computer mouse and the field visualized at the same time. The current software also allows users to visualize the acoustic radiation forces on particles using the model described above. As an alternative to selecting a beamforming operation, the user can manually change the initial phase and amplitude of the transducers to explore the effect on the field. Finally, the transducers are assigned communication channels and the software generates the control signals required for the driver boards.

The software was developed in Java 1.8 to facilitate multiplatform use and access to an Integrated Development Environment that is open. OpenGL was used to render the 3-D graphics and GLSL 3.0 was used to plot the acoustic fields. In the Supplementary Movies, there are examples of how to perform the actions presented in this paper. In the following sections, specific actions of the software are described in more detail.

1) Define the Array Geometry: Defining the array geometry consists of setting the position and orientation of the transducers. First, the aperture of the radiating pistons, the frequency, and the output amplitude constant are set for simulating the generated acoustic field. It is possible to use preset arrays such as flat, hexagonal, or radial (Fig. 2). Another possibility is to import the array geometry from a CSV file or from an OBJ file generated with 3-D modeling software. In Fig. 3, we show the imported geometry from TinyLev [21]. Once imported, the transducers can be moved, rotated, or scaled by the user in real time.

2) Create Foci and Traps: Once the transducers have been positioned, it is possible to change their amplitude and phase to create different acoustic fields. Although the user can set the amplitude and phase manually, the simplest way of working is by creating foci or traps at different points. One option is to click on a slice and the transducers phases will be set to achieve a focus at the target point. The focusing calculation uses a simple geometric ray model. Another option is to enter the coordinates of a control point [green sphere in Fig. 3(b)] and command the software to focus at that point; then, when the point is moved, the array is automatically refocused at the required point. It is possible to store animations that can be played back later at different speeds. The available predefined beamforming operations are: focus point, twin trap with different azimuthal angles, and vortex beams of different topological charges (Fig. 4).

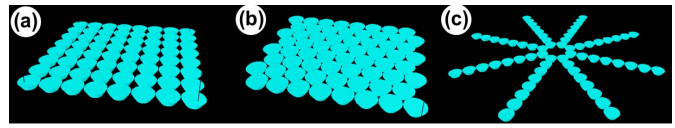

Fig. 2. Preset geometries available. (a) Square grid. (b) Hexagonal grid. (c) Radial.

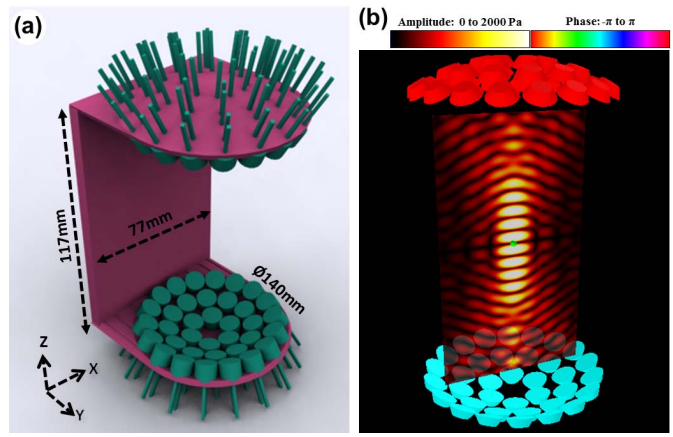

Fig. 3. Importing the array from an OBJ file. (a) Render of the model. (b) Transducers imported into the simulation, the color of the transducers represents their emitting phase; a slice of the amplitude field is presented with a particle placed in one of the nodes.

3) Simulated Acoustic Field and Forces on Particles: It is possible to position 2-D slices on which either the amplitude or the phase is displayed (Fig. 4). The slices will display the field in real time as the transducer positions, phases or amplitudes are changed. The slices themselves can also be moved and rotated around the 3-D space.

For the calculations of acoustic radiation forces on particles some additional parameters are required: density of the host medium (e.g., air) as well as the speed of sound and density of the particle (e.g., EPS). The forces acting on the 1-mm-diameter EPS particle from Fig. 3(b) is shown in Fig. 5.

4) Control of the Driver Boards: The phases and amplitudes calculated in Section II-B2 can now be used to control a driver board that is connected to a computer through the USB: the driver board in turn is connected to the array elements. The software can either send individual frames or a set of frames together with a script that will indicate exactly how many periods of each frame to play. This last operation allows the user to program accurate dynamic field manipulation and modulation options. While the software is designed to interface with the driver board presented in Section II-C, the code has been designed to provide easy integration with other existing and future driver boards.

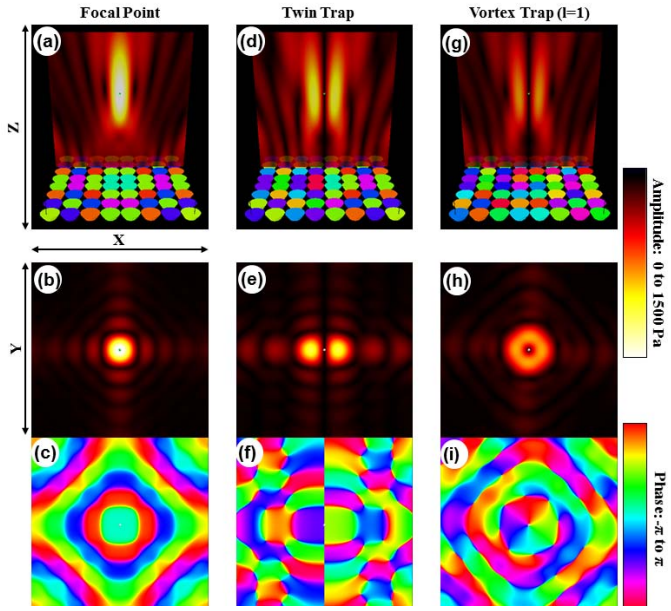

Fig. 4. Different fields generated with a flat 8 × 8 array. (a)–(c) Focus point. (d)–(f) Twin Trap. (g)–(i) Vortex Trap of topological charge $l = 1$. (a), (b), (d), (e), (g), and (h) Amplitude fields. (c), (f), and (i) Phase fields. (a), (d), and (g) Front View. (b), (c), (e), (f), (h), and (i) Top View.

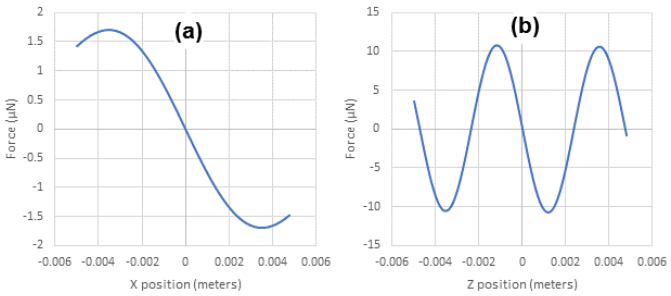

Fig. 5. Simulated force exerted on a 1-mm-diameter EPS particle when it is located at the central node of the single-axis levitator shown in Fig. 3 made of 36 elements at each side separated by 11 cm. (a) Lateral force. (b) Longitudinal force. The forces converge showing that trapping is achieved.

Physical channels can be assigned manually to the transducers but we have developed the following simple automatic protocol for this assignment. A small microcontroller (e.g., Arduino Nano) is also connected to the computer. Its ADC is connected to a single transducer (e.g., Murata MA40S4S) which is used as a microphone. This microphone–transducer is placed on top of a transducer from the array as indicated by the software. Then, a key is pressed and the simulation will emit sequentially from all the transducers in the array until the one that has the ADC on top is detected. This way, it is possible to assign all the transducers to a channel without having to carefully examine the connections. Also, automatic corrections for individual differences in phase and amplitude can be made for each transducer.

C. Driver Board

The driver board is composed of an Arduino Mega that generates 64 digital periodic signals with the phase and amplitude defined by the computer, and a shield that amplifies

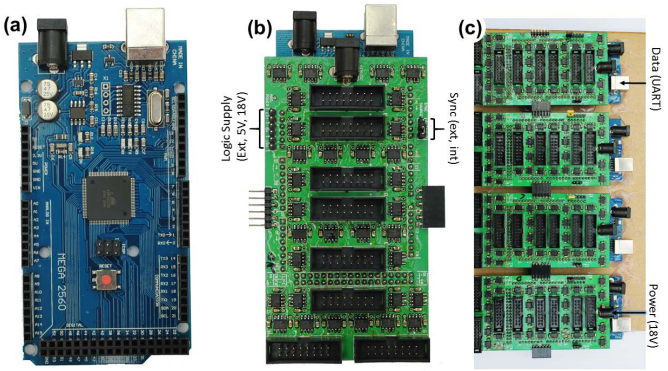

Fig. 6. (a) Arduino Mega used to generate 64 logic signals. (b) Shield mounted on top of the Arduino. The shield amplifies the 64 signals and distributes the sync signal, logic, and power voltage. With the jumpers on the left, the logic supply is selected. (External uses the voltage connected to that pin, 5 V uses the Arduino Power, and 18 V uses the power voltage through the Arduino Voltage regulator.) The jumpers on the right select the source of the sync signal (internal or external). (c) Four boards chained together, the logic supply is set to 18 V and the sync signal is internal for the first board and external for the rest.

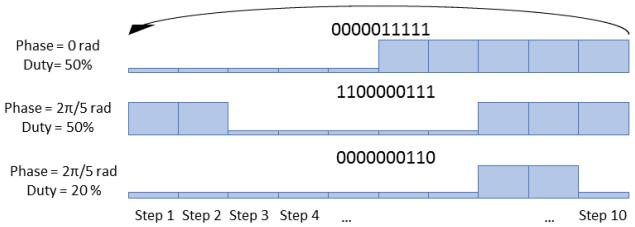

Fig. 7. Controlling amplitude and phase of a half-square wave with a periodic logic digital signal that is divided into ten steps.

these signals up to 17 Vpp. Several driver boards can be chained together to increase the number of channels. In Fig. 6, we show the Arduino Mega, the amplification shield and four boards chained together. In Supplementary Movie 1, we present a step-by-step guide for assembling a driver board.

1) Signal Generation: The Arduino generates 64 digital signals, each signal is represented by a stream of 0s and 1s emitted through a digital output. A pattern of signals is divided into a discrete number of steps that are emitted in a loop fashion, different phases are obtained by shifting the patterns; also, the duty cycle (i.e., number of 1s) can be used to control the amplitude of the output wave (Fig. 7). Despite using a half-square wave, the output of the transducers was found to be sinusoidal given their resonant nature [22], [23] (Fig. 8). Using square-waves simplifies the electronics and reduces the required digital lines per channel while still permitting the generation of excitation signals that produce acoustic sinusoidal waves with controlled amplitude and phase [24].

The main loop of the program outputs the steps that compose the voltage patterns sent to the amplifier and then to the transducers. To synchronize the iterations of the loop, the Arduino generates a sync signal matched to the acoustic frequency (i.e., 40 kHz) using the internal "Timer1," other frequencies can be selected if the application uses a different frequency. When several boards are chained together, this sync signal is generated by the first board and shared amongst the other boards, otherwise small timing deviations would

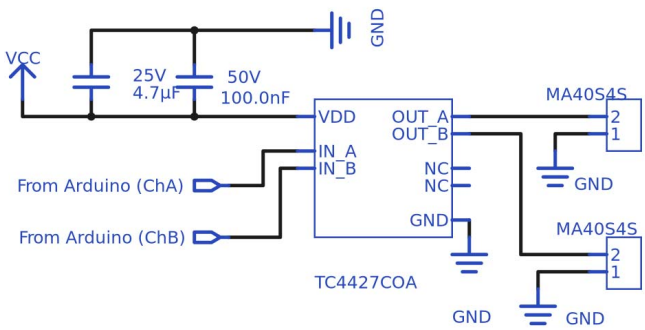

Fig. 8. Logical diagram for two channels of the driver board. This module is repeated 32 times for the whole board.

produce beating effects. During the main loop, the voltage patterns are sequentially sent to the output ports as many times as steps per period are supported. These output operations are intertwined with the operations described in the next paragraphs. No operation instructions were used to calibrate each output step and make them last the same amount of time.

Normally, 64 channels would represent eight ports (1-B each); however, the Arduino Mega has some pins reserved for internal functions so we needed to use ten ports to cover the 64 channels. The maximum supported steps per period at 40 kHz was ten, giving a phase resolution of $\pi/5$; 32 complete voltage patterns (periods) can be stored into the memory of the Arduino.

The boards have two pairs of buffers. One pair is the voltage pattern buffer which contains the patterns that are output in a loop fashion to the ports to generate the excitation signals. The other pair is the duration buffer which specifies how many periods of each pattern should be emitted. It is important to note that a pair of buffers is used in a double buffer scheme so that while new patterns or durations are being received, the old patterns can be emitted with minimum interference.

2) Communication Protocol: The software running on the computer defines the signals that need to be generated by the driver boards. The Arduino Mega receives the commands from the computer using its integrated USB to UART chip. Specifically, the Arduino Mega is connected to the computer by USB and receives data at 250 KBauds, which, using 1-b stop 1-b start, is equivalent to 25 KB/s. When several boards are chained together, the UART output of one board is connected to the input of the next one; the first board input is connected to the computer and the last board output is left unconnected. The boards do not return information to the computer.

Each byte sent by the computer is a command from a simple protocol (Table I). This protocol allows an emission pattern to be added to the pattern buffer, durations to the duration buffer or switch the buffers. The protocol supports up to 15 boards chained together.

The least-significant 4 b of the byte determine the target board; the first board is number 1. If the command has a target board different from 0, the command is for adding emission patterns to the buffer of a specific board. If a board receives a command with 1 as the board number then this board puts the four most-significant bits of the command in its pattern buffer and does not resend the command. Otherwise, the board subtracts 1 from the board number and sends the command to the next board. This way, the control software can add emit patterns to the buffer of specific boards (i.e., if the target board is 1, then the pattern is added to the first board; if the target board is 4, the pattern is added into the fourth board).

TABLE I
COMMUNICATION PROTOCOL COMMANDS

MSB	LSB	Command	Effect
0000	0000	Switch Patterns	Switches the emissions buffers of all the boards
xx11	0000	Add Duration	Appends XX to the durations buffer
0001	0000	Switch Durations	All the durations have been set
XXXX	YYYY	Add Patterns	The board number YYYY appends XXXX to the emission buffer

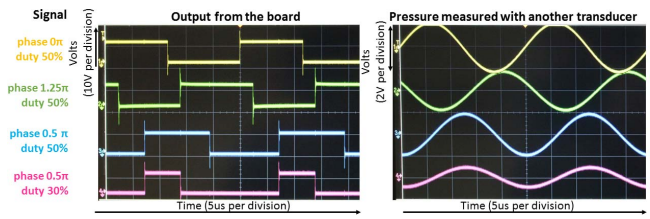

Fig. 9. Signals of different phases and duty cycle generated by the driver board, fed into transducers, and measured with another transducer.

Commands with a target board of 0 are commands for all the boards and are always resent to the next board. These commands are: switch patterns (0b00000000), to indicate that the pattern buffer should we switched so that the new patterns are emitted; Add Duration (0bXX110000), in which the two most-significant bits are used to fill in a duration buffer; and Switch Durations (0b00010000), to switch the duration buffer.

3) Signal Amplification: The logic signals generated by the Arduino MEGA are 5 Vpp but most transducers operate at up to ≈20 Vpp. Therefore, to excite the transducers with enough voltage (and power) it is necessary to amplify the logic signals. We designed a shield that slots on top of the Arduino and amplifies each of the 64 signals to up to 17 Vpp. For every two channels, the circuit uses a dual driver MOSFET TC4427 (Microchip) with 2 decoupling caps (0.1 and 4.7 μF) (Fig. 8). The circuit also distributes the power voltage, logic voltage, sync signal, and UART data amongst all the chained boards. In Fig. 9, we show four output signals from the driver board and the corresponding sound waves created by the transducers as received with another transducer placed on top as a microphone.

D. Arrays

In this section, we describe a simple way of assembling wires to connect the driving board to the transducers. We also show how to create different structures for socketing the transducers into various array shapes. In Supplementary Movie 2, it is shown how to create an 8 × 8 flat array.

The amplification shield has 16-way male MOLEX connectors to provide flexibility in the type of arrays that can

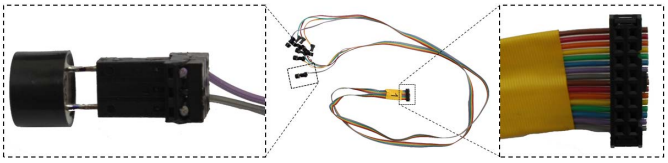

Fig. 10. Wires and connectors used to connect the transducers to the driver boards. 16-way flat ribbon wire is used. A three-way PCB connector is used in the side of the transducers, and a female MOLEX connector is used on the side of the driver board.

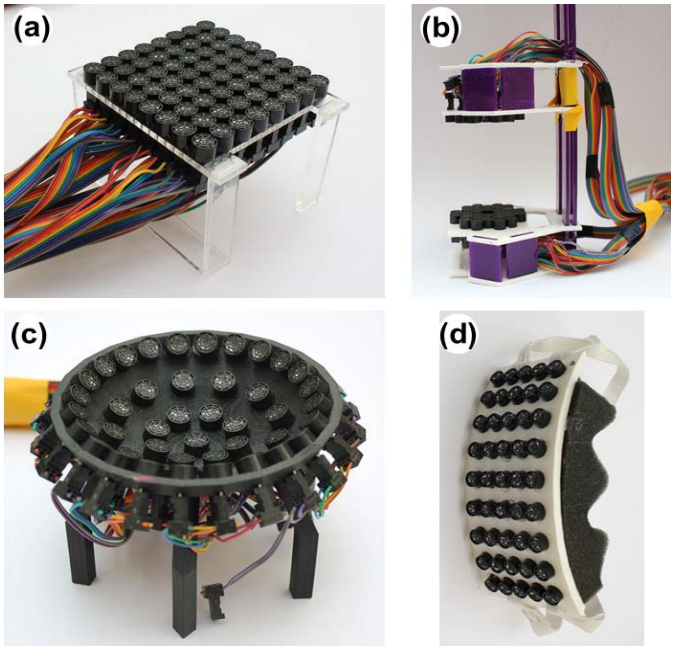

Fig. 11. (a) 8 × 8 flat array mounted in a laser-cut base. (b) Standing-wave levitator with 30 transducers at each side packed in a hexagonal pattern, and with the central transducer removed, the structure was laser cut. (c) 3-D-printed spherical cap with 45 transducers. (d) 3-D-printed curved array with a grid of 9 × 5 transducers.

be connected. We use flat ribbon wires with female MOLEX connectors in the side that connect to the driving board, and three-way PCB connectors to connect to transducers at the other side. The array elements used in the applications discussed in Section III are 10-mm-diameter piezoelectrically actuated transducers (MA40S4S, MURATA, Japan). Note that it is necessary to manually measure their polarity, Marzo *et al.* [23] describes in the Supplementary Movie a simple method for doing so. In Fig. 10, we show eight transducers connected to the ribbon cable.

Laser cutting or 3-D-printing are two options to create the structures in which the transducers are socketed. Laser cutting is efficient and simple for creating flat arrays either single sided or in a standing-wave configuration. 3-D-printing is slower but allows users to create a wider range of shapes such as spherical caps or curved arrays. Example arrays are shown in Fig. 11.

III. Results

A. Generated Fields

In this section, we present a comparison between experimental and simulated fields. The experimental fields were

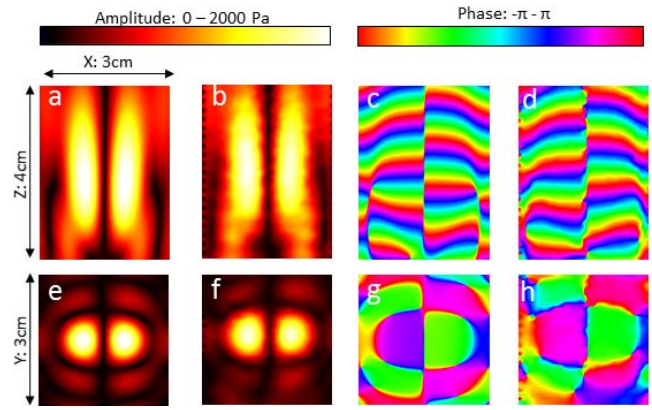

Fig. 12. Twin trap generated 2 cm above the center of an 8 × 8 array. (a), (e), (c), and (g) Simulated fields. (b), (f), (d), and (h) Experimental fields.

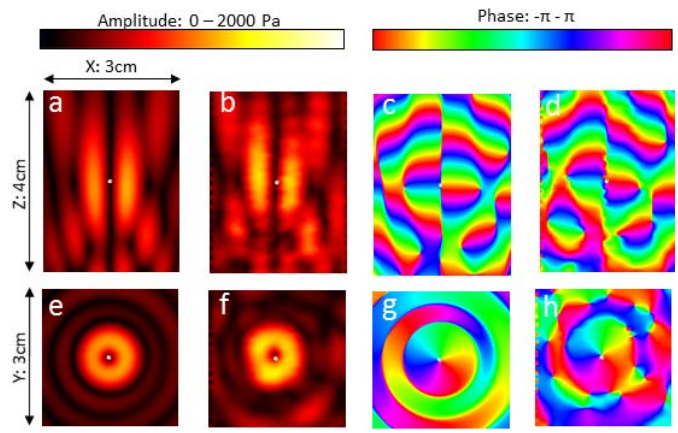

Fig. 13. Voltex-trap generated 2 cm above the center of a spherical cap array. (a), (e), (c), and (g) Simulated fields. (b), (f), (d), and (h) Experimental fields.

scanned with a microphone (1/8" Brüel and Kjær calibrated microphone Type 4138-A-015) attached to a 3-D positioning stage and scanned using a step size of 1 mm. The simulated fields were obtained from the previously described software. In Fig. 12, we show the amplitude and phase field for a Twin-trap generated 2 cm above the flat 8 × 8 array from Fig. 11(a), whereas in Fig. 13, a vortex-trap generated with the spherical cap from Fig. 11(c) is illustrated. It can be seen that the predictions are in a good agreement with the measured field, small deviations may be due to reflections, misalignments, or individual deviations of the transducers (because of the manufacturing processes the transducers do not emit with the same amplitude and phase even when excited with the same signal [21]).

B. Example Applications

In this section, we provide examples of how to use Ultraino for different applications. Full details of all the examples can be seen in the Supplementary Movies.

1) Parametric Loudspeaker: Parametric audio uses ultrasonic fields modulated at audible frequencies to create highly directional audio effects using the sound-from-ultrasound phenomenon. The beam directivity is governed by the ultrasonic frequency and the sound is heard due to nonlinear

effects [25]–[27]. Systems based on this principle have been used to create audio spotlights [28]. With a phased array, the ultrasonic beam can be focused and steered electronically toward a specific region of space or target individual [7], [29]. Such array systems require transmit only operation and use narrow bandwidths centered on the ultrasonic carrier frequency (typically in the range 40–80 kHz).

Here, we use a simple amplitude modulation of the carrier signal with audio. It is appreciated that there are more sophisticated modulation schemes that yield less harmonic distortion [30], and also the modulated audio requires preprocessing in order to optimize the audio quality [31]; however, as this example serves only as a demonstration of the capability of the array and controller, these refinements are omitted.

The flat 8×8 array shown in Fig. 11(a) was used for this example, instead of powering the driver board with a fixed dc, we used the output from an audio amplifier; more specifically, we used the ground and one lead of the outputs from the audio amplifier, we double checked that this signal was always between 0 and 15 V. This is equivalent to applying amplitude modulation on the carrier signal. The result is the generation of audible sound along the ultrasonic beam emitted from the array.

By default, the array outputs with the same phase delay for all the transducers but it is possible to connect to the driver board and use the Ultraino software to electronically steer a focal point while the audio is being played. We generated a focal point 2 m away from the array at different lateral positions to focus the sound at different areas. It was possible to switch the audio between two listeners separated by 2 m. This example can be seen in Supplementary Movie 3.

2) Single-Sided Acoustic Levitation: Phased arrays can generate acoustic fields that exert radiation forces on particles. For instance, this force can be used to paint or sculpt in fur [32] and other artistic media such as sand or liquids [33]. When the acoustic field exerts converging forces, particles can be trapped in mid-air [4]. By changing the phases of the array elements, the field can be modified to move particles in 3-D using four opposed arrays [34]. Later, two opposed arrays were used to create modular systems that represent the trajectory of objects with a levitated particle [35]. It is also possible to levitate particles using single-sided levitators that generate Bessel-shaped tractor beams [36]. Using several levitated particles as graphic representations is an emerging research field [37]. For example, dynamic charts [38] or screens [39] can be created with acoustically levitated particles. The compact size of the available ultrasonic emitters has even led to the development of wearable ultrasonic gloves to manipulate particles in mid-air [40]. All these levitation examples, require a narrowband, transmit-only system with between 50 and 200 elements, the majority operating at 40 kHz.

In this example, we used the 8×8 flat array shown in Fig. 11(a) to generate a twin trap [36] 20 mm above the array. The forces of this trap are converging and thus it is possible to trap a 2-mm-diameter EPS particle in the field (Fig. 14).

Since the wavelength is 8.6 mm, particles of up to 4 mm in diameter can be levitated, i.e., standard acoustic trapping is limited to particles of half-wavelength diameter maximum [41]. In the software, we subsequently changed the position of the trap to move the particle along different paths, this example can be seen in Supplementary Movie 4.

Fig. 14. 8×8 array trapping an EPS Particle 20 mm above the array.

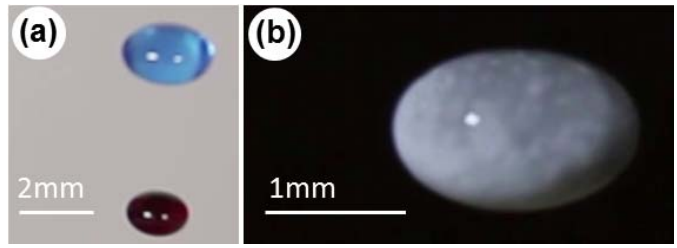

Fig. 15. Standing wave levitating droplets of liquids. (a) Isopropyl alcohol with food coloring. (b) Solution of water and tin dioxide.

3) Standing Wave Levitation: A standing wave was formed between the top and bottom arrays shown in Fig. 3. Particles will be trapped in the nodes of this standing wave. In this case, the trapping strength is larger than in the twin trap in the previous example, so it is possible to levitate liquids. In Fig. 15, we show levitated droplets of isopropyl alcohol and water, this example is shown in Supplementary Movie 5.

4) Ultrasonic Haptic Feedback: The radiation forces of airborne ultrasonic waves can be used to create mid-air haptic sensations. To maximize the effect, the field must be modulated at a frequency perceptible to our mechanoreceptors [42]. This principle has been used to create mid-air tactile displays [5], [43]–[45] and even generate different tactile shapes [46] as the acoustic field is reshaped electronically at high speeds and with sufficient accuracy.

We used a spherical cap array as shown in Fig. 11(c) to generate a focal point 2 cm above the array. We defined an animation with 100 periods with the array on and 100 periods with the array off. By doing so, a focal point is generated and modulated at 200 Hz. Since the mechanoreceptors in our skin are more sensitive to vibrations at this frequency [42], we were able to feel the forces at the focal point with our hand. The focal point can be created at different positions to electronically change where the tactile sensation is applied. This example can be seen in Supplementary Movie 6.

IV. Discussion

In this section, we discuss in more detail the capabilities of Ultraino compared to similar systems and the consequences of some design decisions that were taken. Some research papers can be found about the commercial systems, Ultrahaptics [5], [46], and the Pixie Dust Technologies [7], [37],

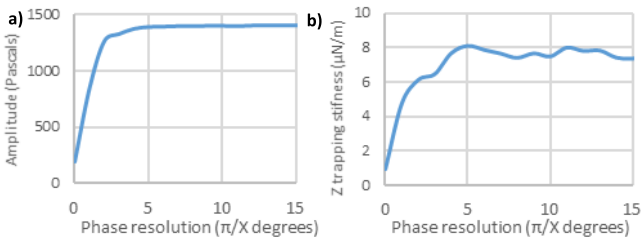

Fig. 16. (a) Amplitude of a focal point created 8 cm above an 8×8 flat array depending on the phase resolution of the driving signals. (b) Trap stiffness on the Z-direction of a twin-trap created 2.5 cm above an 8×8 flat array depending on the phase resolution of the driving signals.

but we note that the system specification may have changed slightly from the published prototypes.

A. Selected Microcontroller

We selected an Arduino Mega as the microcontroller because of the simplicity of programming it, the wide range of existing users, its low price, high number of IOs (72) and integrated UART to USB chip. Other options were a Raspberry PI 2 which costs slightly more, provides only 26 GPIOS and takes around 30 s to boot up.

Alternatively, field-programmable gate array (FPGA) or CPLDs could be used but these are again more expensive options and are more challenging to program. However, FPGAs have a high number of IOs, enabling operation at higher frequencies and providing higher phase resolution. Using individual ICs is a further option to reduce the cost of an FPGA system but assembling all the required parts (e.g., clock or flash memory) adds complexly to the assembly. We note that Ultrahaptics first used 5 XMOS processors (Bristol, UK) and has recently swapped to an FPGA solution; Pixie Dust uses an FPGA making it very hard to reprogram it.

B. Phase Resolution

Ultraino has a phase resolution of $\pi/5°$ when working at 40 kHz with 64 channels. It is possible to obtain higher phase resolutions at lower frequencies or when controlling less channels. The code for a 16-channel board based on Arduino Nano and with $\pi/12°$ of phase resolution is also provided. Ultrahaptics has a phase resolution of $\pi/25$ [46], and the phase resolution for Pixie Dust arrays is $\pi/8$ [37].

A phase resolution of $\pi/5°$ operating at 40 kHz provides a simulated nodal position accuracy of 0.9 mm obtained when moving the node in the levitator shown in Fig. 3. Particle positional accuracy is closely related to nodal positional accuracy; however, the particle is typically displaced from the node by the effects of gravity.

In Fig. 16(a), we show how the amplitude of a focal point generated 8 cm above an 8×8 flat array [Fig. 11(a)] varies depending on the phase resolution. In Fig. 16(b), we illustrate how the trapping force along the direction of propagation of a twin-trap varies with different phase resolutions, the trap is generated 2 cm above an 8×8 array. As it can be seen, there is no major loss from using a phase resolution of $\pi/5$ for focusing the beam or creating traps.

C. Maximum Voltage

The maximum voltage supported by the driver board is 17 Vpp, this limit comes from the MOSFET drivers employed, which are rated at 18 Vpp maximum. Ultrahaptics supports up to 20 Vpp but only when operating in pulse mode. Pixie Dust boards support up to 24 Vpp but requires active cooling in the form of fans. We decided to use one channel of the MOSFET driver per transducer to minimize cost, complexity of soldering and footprint of the board. It would be possible to use two channels in a push–pull configuration to obtain 32 Vpp or to use more expensive MOSFET drivers that can go up to over 40 Vpp per channel. However, we think that using one channel of the TC4427 per channel offers a good balance between maximum voltage, price, board size, and number of components as well as the not necessity of cooling.

When the particles are small compared to the wavelength, the radiation force is proportional to the volume [19]; therefore, levitation is density dependent. The standing-wave levitator can levitate samples of up to 1.1 g/cm^3 density operating at 15 Vpp, whereas the single-sided levitator has only been tested with Styrofoam particles (i.e., 29 Kg/m^3).

D. Update Speed and Pattern Storage

The Ultraino driver board can update the emission patterns for 64 channels 25 times per second using an UART speed of 250 Kbauds, the speed can be increased up to 2 MBauds for updating the board 100 times per second, but the setup becomes more susceptible to interference/error. The UART is favored here as it simplifies the hardware, integration and development process. Ultrahaptics support high-speed rates since it uses USB 2.0, although this increases the complexity of stablishing communication with the board and finding suitable drivers. The update rate of Pixie Dust arrays is 1 kHz [37], it seems that instead of phase patterns the board receives the position of the target focus and they do the calculations on the board, making the system faster but less versatile. Although our boards can only be updated at up to 100 times per second, we provide an option for faster and more accurate field updating. It is possible to upload 32 patterns onto the board as well as a script that specifies exactly how many periods each pattern should be emitted.

E. Number of Boards

Ultrahaptics does not allow the chaining of multiple boards to further increase the number of channels. In Pixie Dust, up to four boards can be chained together since they only need to receive the position of the target focus. In Ultraino, the chained boards share the sync signal and the data channel, so it is still possible to send individual phases to each board. This sync signal is just a clock to mark the 40-kHz reference. So, there is no deviation between the boards other than the one introduced by the signal traveling through the PCB tracks which is negligible at 40 kHz. Up to 15 boards can be chained together but only four chained boards have been tested in a real system.

F. Transducer Position

Ultrahaptics and Pixie Dust arrays have the transducers soldered onto the PCB. This simplifies its production since

they avoid the use of connectors and wires. However, for a research platform it is important to maximize flexibility by enabling users to position the transducers arbitrarily to create curved arrays or other types of geometries.

V. Conclusion

We have described an open platform for defining, simulating and controlling narrowband phased-arrays operating in transmission at 40 kHz in air; both the software and hardware are open. Example applications have been shown in parametric loudspeakers, acoustic levitation, and mid-air ultrasonic haptic feedback. This demonstrates that the Ultraino system has the capability to inexpensively and quickly allow researchers to explore a range of new airborne ultrasound application. We hope that Ultraino allows researchers and ultrasound enthusiasts to explore these and future novel scenarios.

References

[1] C. Pell, "Phased-array radars," *IEE Rev.*, vol. 34, no. 9, pp. 363–367, 1988.

[2] J. H. G. Ender and A. R. Brenner, "PAMIR—A wideband phased array SAR/MTI system," *IEE Proc.-Radar, Sonar Navigat.*, vol. 150, no. 3, pp. 165–172, 2003.

[3] B. W. Drinkwater and P. D. Wilcox, "Ultrasonic arrays for non-destructive evaluation: A review," *NDT E Int.*, vol. 39, no. 7, pp. 525–541, Oct. 2006.

[4] E. H. Brandt, "Acoustic physics: Suspended by sound," *Nature*, vol. 413, no. 6855, pp. 474–475, Apr. 2001.

[5] T. Carter, S. A. Seah, B. Long, B. Drinkwater, and S. Subramanian, "UltraHaptics: Multi-point mid-air haptic feedback for touch surfaces," in *Proc. 26th Annu. ACM Symp. User Interface Softw. Technol. (UIST)*, 2013, pp. 505–514.

[6] M. Perry, "Receiver communications for wireless power transfer," U.S. Patent 9 001 622 B2, Apr. 7, 2015.

[7] Y. Ochiai, T. Hoshi, and I. Suzuki, "Holographic whisper: Rendering audible sound spots in three-dimensional space by focusing ultrasonic waves," in *Proc. CHI Conf. Human Factors Comput. Syst. (CHI)*, 2017, pp. 4314–4325.

[8] J. A. Jensen *et al.*, "Ultrasound research scanner for real-time synthetic aperture data acquisition," *IEEE Trans. Ultrason., Ferroelect., Freq. Control*, vol. 52, no. 5, pp. 881–891, May 2005.

[9] P. R. Smith, D. M. J. Cowell, B. Raiton, C. V. Ky, and S. Freear, "Ultrasound array transmitter architecture with high timing resolution using embedded phase-locked loops," *IEEE Trans. Ultrason., Ferroelect., Freq. Control*, vol. 59, no. 1, pp. 40–49, Jan. 2012.

[10] E. Boni *et al.*, "ULA-OP 256: A 256-channel open scanner for development and real-time implementation of new ultrasound methods," *IEEE Trans. Ultrason., Ferroelect., Freq. Control*, vol. 63, no. 10, pp. 1488–1495, Oct. 2016.

[11] J. A. Jensen *et al.*, "Experimental ultrasound system for real-time synthetic imaging," in *Proc. IEEE Ultrason. Symp. Int. Symp.*, Oct. 1999, pp. 1595–1599.

[12] J. A. Jensen *et al.*, "Performance of SARUS: A synthetic aperture real-time ultrasound system," in *Proc. IEEE Int. Ultrason. Symp.*, Oct. 2010, pp. 305–309.

[13] C. A. Winckler, P. R. Smith, D. M. J. Cowell, O. Olagunju, and S. Freear, "The design of a high speed receiver system for an ultrasound array research platform," in *Proc. IEEE Int. Ultrason. Symp.*, Oct. 2012, pp. 1481–1484.

[14] T. Wilson, J. Zagzebski, T. Varghese, Q. Chen, and M. Rao, "The ultrasonix 500RP: A commercial ultrasound research interface," *IEEE Trans. Ultrason., Ferroelect., Freq. Control*, vol. 53, no. 10, pp. 1772–1782, Oct. 2006.

[15] P. Tortoli, L. Bassi, E. Boni, A. Dallai, F. Guidi, and S. Ricci, "ULA-OP: An advanced open platform for ultrasound research," *IEEE Trans. Ultrason., Ferroelect., Freq. Control*, vol. 56, no. 10, pp. 2207–2216, Oct. 2009.

[16] E. Boni *et al.*, "A reconfigurable and programmable FPGA-based system for nonstandard ultrasound methods," *IEEE Trans. Ultrason., Ferroelect., Freq. Control*, vol. 59, no. 7, pp. 1378–1385, Jul. 2012.

[17] S. Harput, A. Bozkurt, and F. Y. Yamaner, "Ultrasonic phased array device for real-time acoustic imaging in air," in *Proc. IEEE Ultrason. Symp.*, Nov. 2008, pp. 619–622.

[18] H. T. O'Neil, "Theory of focusing radiators," *J. Acoust. Soc. Amer.*, vol. 21, no. 5, pp. 516–526, 1949.

[19] L. P. Gorkov, "Forces acting on a small particle in an acoustic field within an ideal fluid," *Doklady Akademii Nauk Sssr*, vol. 140, no. 1, p. 88, 1961.

[20] T. Iwamoto, M. Tatezono, and H. Shinoda, "Non-contact method for producing tactile sensation using airborne ultrasound," in *Proc. Euro-Haptics, Perception, Devices Scenarios*, 2008, pp. 504–513.

[21] A. Marzo, A. Barnes, and B. W. Drinkwater, "TinyLev: A multi-emitter single-axis acoustic levitator," *Rev. Sci. Instrum.*, vol. 88, no. 8, p. 085105, 2017.

[22] S. A. Seah, B. W. Drinkwater, T. Carter, R. Malkin, and S. Subramanian, "Correspondence: Dexterous ultrasonic levitation of millimeter-sized objects in air," *IEEE Trans. Ultrason., Ferroelect., Freq. Control*, vol. 61, no. 7, pp. 1233–1236, Jul. 2014.

[23] A. Marzo, A. Ghobrial, L. Cox, M. Caleap, A. Croxford, and B. W. Drinkwater, "Realization of compact tractor beams using acoustic delay-lines," *Appl. Phys. Lett.*, vol. 110, no. 1, p. 014102, Feb. 2017.

[24] P. R. Smith, D. M. J. Cowell, and S. Freear, "Width-modulated square-wave pulses for ultrasound applications," *IEEE Trans. Ultrason., Ferroelect., Freq. Control*, vol. 60, no. 11, pp. 2244–2256, Nov. 2013.

[25] F. J. Pompei, "The use of airborne ultrasonics for generating audible sound beams," in *Proc. Audio Eng. Soc. Conv.*, vol. 105. 1998, paper 4853.

[26] H. O. Berktay, "Possible exploitation of non-linear acoustics in underwater transmitting applications," *J. Sound Vibrat.*, vol. 2, no. 4, pp. 435–461, 1965.

[27] E. A. Zabolotskaya, "Quasiplane waves in the nonlinear acoustics of confined beams," *Soviet Phys. Acoust.*, vol. 15, pp. 35–40, Jan. 1969.

[28] M. Yoneyama, J.-I. Fujimoto, Y. Kawamo, and S. Sasabe, "The audio spotlight: An application of nonlinear interaction of sound waves to a new type of loudspeaker design," *J. Acoust. Soc. Amer.*, vol. 73, no. 5, pp. 1532–1536, 1983.

[29] A.-C. Bourland, P. Gorman, J. Mcintosh, and A. Marzo, "Project telepathy: Targeted verbal communication using 3D beamforming speakers and facial electromyography," in *Proc. CHI Conf. Extended Abstracts Human Factors Comput. Syst. (CHI EA)*, 2017, pp. 1508–1515.

[30] E.-L. Tan, P. Ji, and W.-S. Gan, "On preprocessing techniques for bandlimited parametric loudspeakers," *Appl. Acoust.*, vol. 71, no. 5, pp. 486–492, 2010.

[31] T. D. Kite, J. T. Post, and M. F. Hamilton, "Parametric array in air: Distortion reduction by preprocessing," *J. Acoust. Soc. Amer.*, vol. 103, no. 5, p. 2871, 1998.

[32] Y. Sugiura, K. Toda, T. Hoshi, Y. Kamiyama, T. Igarashi, and M. Inami, "Graffiti fur: Turning your carpet into a computer display," in *Proc. 27th Annu. ACM Symp. User Interface Softw. Technol. (UIST)*, 2014, Art. no. 9.

[33] A. Marzo, R. Mcgeehan, J. Mcintosh, S. A. Seah, and S. Subramanian, "Ghost touch: Turning surfaces into interactive tangible canvases with focused ultrasound," in *Proc. Int. Conf. Int. Tabletops Surfaces (ITS)*, 2015, pp. 137–140.

[34] Y. Ochiai, T. Hoshi, and J. Rekimoto, "Three-dimensional mid-air acoustic manipulation by ultrasonic phased arrays," *PLoS ONE*, vol. 9, no. 5, p. e97590, 2014.

[35] T. Omirou, A. Marzo, S. A. Seah, and S. Subramanian, "LeviPath: Modular acoustic levitation for 3D path visualisations," in *Proc. 33rd Annu. ACM Conf. Human Factors Comput. Syst. (CHI)*, 2015, pp. 309–312.

[36] A. Marzo, S. A. Seah, B. W. Drinkwater, D. R. Sahoo, B. Long, and S. Subramanian, "Holographic acoustic elements for manipulation of levitated objects," *Nature Commun.*, vol. 6, p. 8661, May 2015.

[37] Y. Ochiai, T. Hoshi, and J. Rekimoto, "Pixie dust: Graphics generated by levitated and animated objects in computational acoustic-potential field," *ACM Trans. Graph.*, vol. 33, no. 4, 2014, Art. no. 85.

[38] T. Omirou, A. M. Perez, S. Subramanian, and A. Roudaut, "Floating charts: Data plotting using free-floating acoustically levitated representations," in *Proc. IEEE Symp. 3D User Interfaces (3DUI)*, Mar. 2016, pp. 187–190.

[39] D. R. Sahoo, T. Nakamura, A. Marzo, T. Omirou, M. Asakawa, and S. Subramanian, "JOLED: A mid-air display based on electrostatic rotation of levitated janus objects," in *Proc. 29th Annu. Symp. User Interface Softw. Technol. (UIST)*, 2016, pp. 437–448.

[40] A. Marzo, "GauntLev: A wearable to manipulate free-floating objects," in *Proc. CHI Conf. Human Factors Comput. Syst. (CHI)*, 2016, pp. 3277–3281.
[41] D. Zang, K. Lin, L. Li, Z. Chen, X. Li, and X. Geng, "Acoustic levitation of soap bubbles in air: Beyond the half-wavelength limit of sound," *Appl. Phys. Lett.*, vol. 110, no. 12, p. 121602, 2017.
[42] L. Gavrilov, E. Tsirulnikov, and I. I. Davies, "Application of focused ultrasound for the stimulation of neural structures," *Ultrasound Med. Biol.*, vol. 22, no. 2, pp. 179–192, 1996.
[43] H. Bruus, "Acoustofluidics 7: The acoustic radiation force on small particles," *Lab Chip*, vol. 12, no. 6, pp. 1014–1021, 2012.
[44] T. Hoshi, M. Takahashi, T. Iwamoto, and H. Shinoda, "Noncontact tactile display based on radiation pressure of airborne ultrasound," *IEEE Trans. Haptics*, vol. 3, no. 3, pp. 155–165, Jul./Sep. 2010.
[45] Y. Ochiai, K. Kumagai, T. Hoshi, S. Hasegawa, and Y. Hayasaki, "Cross-field aerial haptics: Rendering haptic feedback in air with light and acoustic fields," in *Proc. CHI Conf. Human Factors Comput. Syst. (CHI)*, 2016, pp. 3238–3247.
[46] B. Long, S. A. Seah, T. Carter, and S. Subramanian, "Rendering volumetric haptic shapes in mid-air using ultrasound," *ACM Trans. Graph.*, vol. 33, no. 6, 2014, Art. no. 181.

Asier Marzo received the B.Eng. degree in computer science, the M.Sc. degree in information technologies, and the Ph.D. degree in computer science from the Public University of Navarre, Pamplona, Spain, in 2009, 2011, and 2016, respectively. His doctoral dissertation was about the use of holographic elements for acoustic levitation.

He is currently a Research Assistant with the Department of Mechanical Engineering, Bristol University, Bristol, U.K. His current research interests include serious games for education, mobile augmented reality, and the tangible effects of waves in matter.

Tom Corkett received the M.Eng. degree (First Class Hons.) in electrical and electronic engineering from University of Bristol, Bristol, U.K., in 2017.

He was an Intern at the University of Melbourne, Melbourne, VIC, Australia, where he was involved in the development of a power system for the CubeSat satellite of the Melbourne Space Program. He was with the University of Bristol, Bristol, U.K., where he was involved in the development of an Internet-of-Things device for logging over Bluetooth the variations in the oscillation of a clock pendulum. In 2017, he joined the Cyber Security branch, PwC, London, U.K. His current research interests include PCB design, cyber security, and integrated systems.

Bruce W. Drinkwater received the B.Eng. and Ph.D. degrees in mechanical engineering from Imperial College, London, U.K., in 1991 and 1995, respectively.

Since 1996, he has been with the Mechanical Engineering Department, University of Bristol, Bristol, U.K., where he became a Professor of ultrasonics in 2007. He was involved in the interaction of ultrasound with adhesive joints, thin layers, and interfaces, ultrasonic array imaging, where the techniques he developed are now widely used in industry, and acoustic radiation force devices for micro- and macroscale applications.

Dr. Drinkwater received the Roy Sharpe Award for his contribution to nondestructive testing, in 2010 and a Royal Society Wolfson Research Merit Award in 2017.